Analysis of Multi-Layer Integrated Inductors with Wave Concept Iterative Procedure (WCIP)

S. Akatimagool*, D. Bajon* and H. Baudrand**

*SUPAERO., 10, av. Edouard Belin, 31055, Toulouse, France, Tel : (+33) 5 62 17 80 81
**ENSEEIHT., 2, rue Camichel, 31071, Toulouse, France, Tel : (+33) 5 61 58 82 46

***Abstract* - In this paper, we present the WCIP iterative procedure (Wave Concept Iterative Procedure) for solving continuity conditions in terms of waves rather than in term of tangential fields providing a mixed resolution in spatial and spectral domain taking the best advantage of each resolution domain and lower computation time. The spiral inductor with patterned ground shield is taken as an example of multi-layer structures; the results are in reasonably good agreement with the experimental data.**

I. INTRODUCTION

Silicon-based technology offers many design parameters to conceive passive elements in particular the different interconnect levels allowing optimized conceptions [1-5]. For simulations in the spatial domain, thin multi-layer stacks are responsible of highly increased calculation complexity. We will focus in this work on spiral inductors with patterned ground shield and on their modeling with the Wave Concept Iterative Procedure (WCIP) [6]. Spatial domain provides the versatility in circuit description while spectral domain ensures reliable description of multi-layer substrates.

II. GENERAL THEORY

The efficiency of WCIP is mainly result of the building of an iterative procedure, which avoids the inversion of the integral operator to solve the boundary conditions problem owing to its waves based formulation.

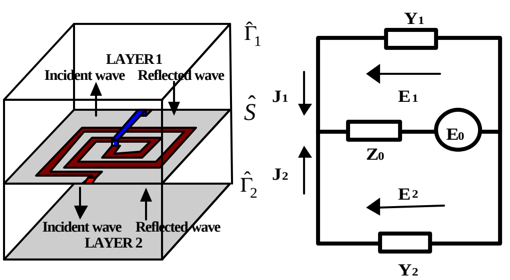

Fig. 1 The ideal WCIP structure and the equivalent electromagnetic circuit

A. Definition of the waves

According to the surface S in Fig. 1, the waves are defined as a linear combination of the tangential fields as :

$$\left.\begin{aligned} A &= \frac{1}{2\sqrt{Z_0}}\left(E_t + Z_0 H_t \wedge n\right) \\ B &= \frac{1}{2\sqrt{Z_0}}\left(E_t - Z_0 H_t \wedge n\right) \end{aligned}\right\} \qquad (1)$$

with Z_0 an arbitrary wave impedance, E_t and H_t the electric and magnetic tangential fields to the surface and *n* the outgoing normal to the surface.

B. Boundary continuity conditions in terms of waves

On the printed surfaces, the boundary conditions on tangential fields are translated in terms of waves ; on the metallic sub-domain D_M, the cancellation condition of tangential electric fields $E_1 = E_2 = 0$ (the subscript *i=1,2* refers to the two sides of the printed surface) yields, from the definition (1), the following S matrix to represent the continuity conditions :

$$\begin{bmatrix} B_1 \\ B_2 \end{bmatrix}_M = \begin{bmatrix} -1 & 0 \\ 0 & -1 \end{bmatrix} \begin{bmatrix} A_1 \\ A_2 \end{bmatrix}_M \qquad (2)$$

On the dielectric sub-domain D_D, the conditions $E_1 = E_2$ and $J_1 + J_2 = 0$ give :

$$\begin{bmatrix} B_1 \\ B_2 \end{bmatrix}_D = \begin{bmatrix} \frac{1-n^2}{n^2+1} & \frac{2n}{n^2+1} \\ \frac{2n}{n^2+1} & \frac{n^2-1}{n^2+1} \end{bmatrix} \begin{bmatrix} A_1 \\ A_2 \end{bmatrix}_D \qquad (3)$$

while, on the source sub-domain D_S, $E_1 = E_0 - Z_0(J_1 + J_2)$ give :

$$\begin{bmatrix} B_1 \\ B_2 \end{bmatrix}_S = \begin{bmatrix} \frac{-1+n_1-n_2}{1+n_1+n_2} & \frac{2n_{12}}{1+n_1+n_2} \\ \frac{2n_{12}}{1+n_1+n_2} & \frac{-1-n_1+n_2}{1+n_1+n_2} \end{bmatrix} \begin{bmatrix} A_1 \\ A_2 \end{bmatrix}_S \qquad (4)$$

where $n = \sqrt{\frac{Z_1}{Z_2}}$, $n_{12} = \frac{Z_0}{Z_1 Z_2}$, $n_1 = \frac{Z_0}{Z_1}$ and $n_2 = \frac{Z_0}{Z_2}$.

C. Integral operator in the spectral domain

As far as separable geometry is concerned, the set of functions associated to both TE and TM transverse electric fields provides a complete set of orthogonal basis functions suitable to expand electric fields in the boxed structure as [6-7]:

$$\boldsymbol{E}_T(x,y) = \sum_{a,m,n} a^{a}_{m,n} f^{a}_{m,n}(x,y) \qquad (5)$$

in which α denotes the TE and TM mode functions. The magnetic field is expressed as :

$$\boldsymbol{J}(x,y) = \boldsymbol{H}(x,y)\times \boldsymbol{n} = \sum_{a,m,n} a^{a}_{m,n} Y^{a}_{m,n} f^{a}_{m,n}(x,y) \qquad (6)$$

The expressions (5) and (6) support the expansion in the spectral domain of the integral operator $\hat{Y}$ defined as :

$$J = \hat{Y}E \quad \text{with} \quad \hat{Y} = \sum_{a,m,n} \left| f^{a}_{m,n} \right\rangle Y^{a}_{m,n} \left\langle f^{a}_{m,n} \right| \qquad (7)$$

Hence, from definition (1), the waves can be expanded on the same set of basis functions than the tangential fields and the $\hat{\Gamma}_i$ operator such that $B_i = \hat{\Gamma} A_i$, where $i = 1,2$ refers to the sides of surface S, has the general form :

$$\hat{\Gamma}_i = \sum_{m,n} \left| f^{a}_{m,n} \right\rangle \Gamma^{a}_{m,n} \left\langle f^{a}_{m,n} \right| \qquad (8)$$

Applying $\hat{\Gamma}$ simply consists in multiplying the modal amplitude of the waves by the corresponding numbers Γ_i^{TE} and Γ_i^{TM} in (8), such that

$$\Gamma^{a}_{i\,m,n} = \frac{1 - Z_{0i} Y^{a}_{i\,m,n}}{1 + Z_{0i} Y^{a}_{i\,m,n}} \qquad (9)$$

D. Integral operators in multi-layer structures

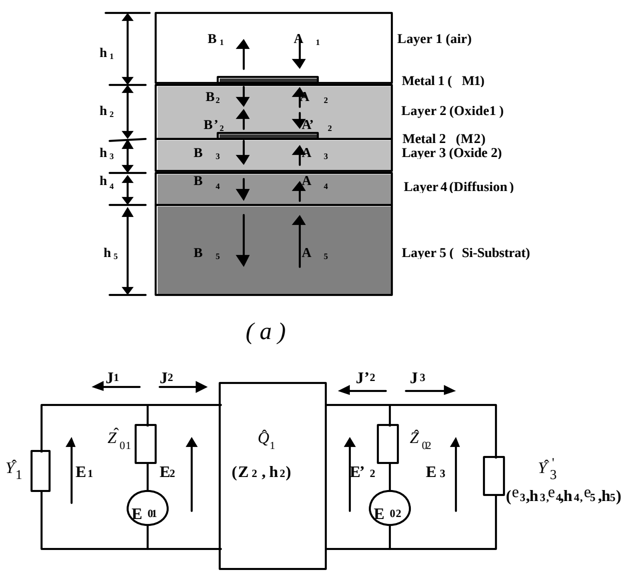

Fig. 2 Typical multilayer structure (a) and the equivalent electromagnetic circuit of the problem (b).

The relations between the waves on each printed layers are sketched in the equivalent electromagnetic circuit in Fig. 2-b by the integral operators $\hat{Y}_1$, $\hat{Y}'_3$ and $\hat{Q}_1$ related respectively to the upper half space, the substrate under the M2 metal level and the oxide between the metal 1 (M1) and the metal 2 (M2). All of these operators are handled through their reflection coefficient-like version whose spectral expansion form is given in (8).

The modal admittance, Y'_{3mn} used in (7) to build the operator form (9) of $\hat{Y}'_3$ is given by :

$$Y'_{5m,n} = Y_{5m,n}\cosh(g_{5m,n}h_5)$$

$$Y'_{4m,n} = Y_{4m,n}\left(\frac{Y'_{5m,n} + Y_{4m,n}\tanh(g_{4m,n}h_4)}{Y_{4m,n} + Y'_{5m,n}\tanh(g_{4m,n}h_4)}\right)$$

$$Y'_{3m,n} = Y_{3m,n}\left(\frac{Y'_{4m,n} + Y_{3m,n}\tanh(g_{3m,n}h_3)}{Y_{3m,n} + Y'_{4m,n}\tanh(g_{3m,n}h_3)}\right)$$

with $g_{im,n} = \sqrt{\frac{m^2p^2}{a^2} + \frac{n^2p^2}{b^2} - k_0^2 e_{ri}}$, $i = 1,2,3,..$ refers to the layer i, a and b to the dimensions of the calculation box and $Y_{im,n}$ the mode admittance of modes m, n.

The two port operator $\hat{Q}_1$ has a spectral expansion in the following form :

$$\hat{S}_Q = \sum_{m,n}\begin{bmatrix} \left| f^{a}_{m,n}\right\rangle \frac{\left(Z_2^2 - Z_{01}Z_{02}\right)\sinh\left(g_{m,n}h_2\right)}{H}\left\langle f^{a}_{m,n}\right| & \left| f^{a}_{m,n}\right\rangle \frac{2Z_2\sqrt{Z_{01}Z_{02}}}{H}\left\langle f^{a}_{m,n}\right| \\ \left| f^{a}_{m,n}\right\rangle \frac{2Z_2\sqrt{Z_{01}Z_{02}}}{H}\left\langle f^{a}_{m,n}\right| & \left| f^{a}_{m,n}\right\rangle \frac{\left(Z_2^2 - Z_{01}Z_{02}\right)\sinh\left(g_{m,n}h_2\right)}{H}\left\langle f^{a}_{m,n}\right| \end{bmatrix}$$

with $H = 2Z_2\sqrt{Z_{01}Z_{02}}\cosh(g_{m,n}h_2) + \left(Z_2^2 + Z_{01}Z_{02}\right)\sinh(g_{m,n}h_2)$.

E. Iterative procedure

The whole printed surface being discretized by pixel-like functions, collecting for each sub-domain the S-relations (2-4) described in the previous section, the scheme of the successive iterations is given by :

$$\left.\begin{aligned} B &= \hat{S}\,A + B_0 && \textit{in the spatial domain} \\ A &= \hat{\Gamma}B && \textit{in the spectral domain} \end{aligned}\right\} \qquad (10)$$

The toggling between the spatial and the spectral representation of the waves A and B is ensured by a fast modal transform quite similar to the fast Fourier transform which takes advantages in the pixel-like discretization of the printed surface (see flowchart 1).

Let P be the number of pixels and N the number of iterations, the total number of operations N_T for a simulation is given by :

$$N_T = 4NP(\,1 + 3\ln P\,) \qquad (11)$$

while usual moment methods require $(KP)^3/3$ operations with K being the ratio between the metallic part of the circuit and the total surface.

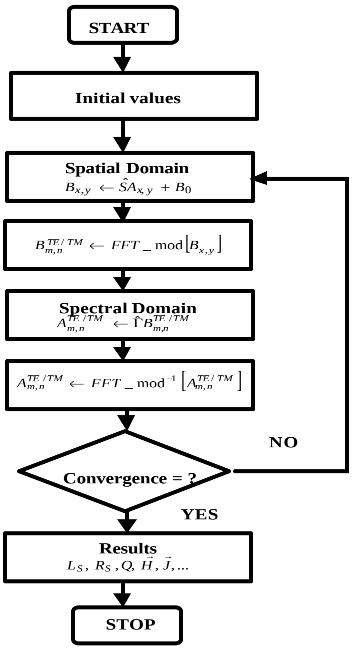

Flowchart 1 The iterative procedure of the waves

III. Modeling Of The Spiral Inductance

The equivalent circuit of a spiral inductor on silicon substrate is shown in fig. 3.

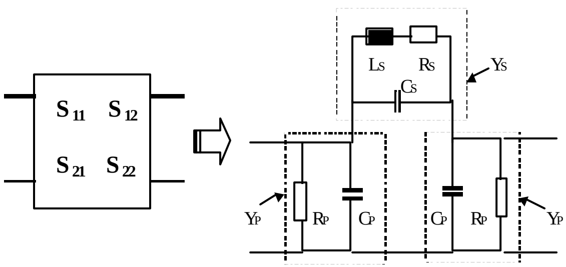

Fig. 3 The equivalent circuit of the spiral inductor

The lumped elements in the π-network of the spiral inductor are extracted from the calculated scattering matrix and the quality factor of the spiral inductance is deduced by the expression given by Yue and Wong [3].

IV. Numerical Results

The nominal technological parameters of the one turn and half self Inductance in Fig. 4-b considered in this work are 20 Ω-cm silicon substrate with a 1.5 µm thick diffusion layer, 0.5 µm and 6 µm of oxide, respectively. The metal thickness of the inductor is 3 µm with conductivity of $3.3*10^7$ S/m. The conductors and the line spacing are 26 µm and 8.66 µm wide, respectively, the overall dimensions are 260*260 µm². The patterned ground shield is fabricated using 0.3 µm thick poly-Silicon. The spiral and the ground shield are separated by 6 µm oxide. After WCIP calculation, current density and electric field are in readily obtained. The magnitude of the electric field distribution on the inductor layer and the patterned ground shield layer is displayed in Fig. 5

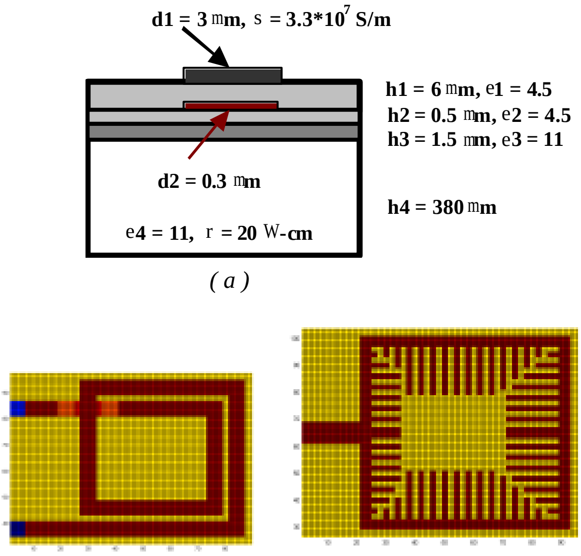

(a) (b) (c)

Fig. 4 (a) Modeling of the multi-layer circuit, (b) meshing of the printed structure of the spiral inductor and, (c) Patterned ground shield

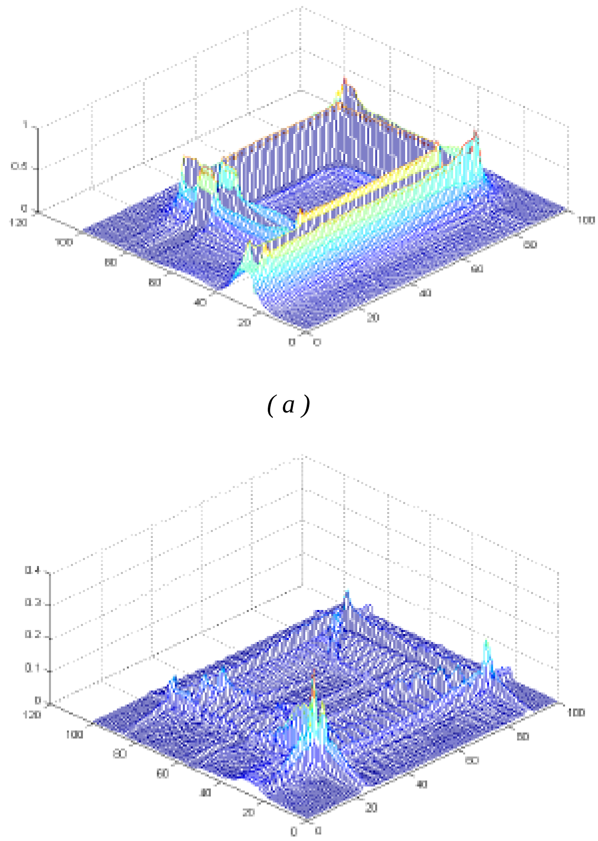

(a)

(b)

Fig. 5 Computed electric field distribution (a) on the inductor and, (b) on the patterned ground shield layer

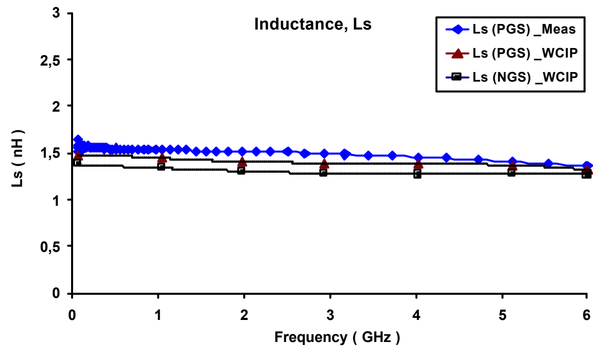

(a)

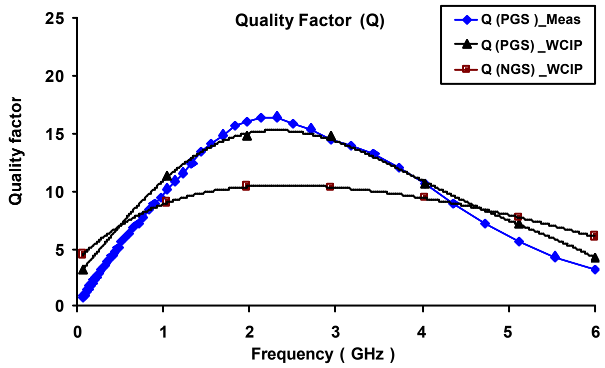

(b)

Fig.6 Comparison of the experimental results and the simulation (WCIP)) with Patterned Ground Shield (PGS) and No Ground Shield (NGS) (a) inductance and, (b) quality factor

TABLE 1

Comparison of the experimental results and the simulation (WCPI)) with Patterned Ground Shield (PGS) and No Ground Shield (NGS)

Results	Measure (PGS)	WCIP (PGS)	WCIP (NGS)
Q_{max}	16.45	15.3	10.5
L_S (nH)	1.50	1.42	1.28
R_S (W)	1.2	0.92	1.3
C_S (fF)	13.5	12	12
R_p (kW)	3.80	1.20	0.68
Cp (fF)	258	145	127
f_{Qmax} (GHz)	2.3	2.3	2.3

In Fig.6 and Table 1 the results are confronted to measurements and the influence of patterned shield is outlines and shows a Q-factor improvement of around 5 units in comparison with the bottom ground plane case.

Fig.7 presents a comparison between the number of operations (N_T) in standard Moment Method (MOM) and WCIP for different numbers of iterations in equation (11). WCIP is indeed seen as a good candidate to introduce for example grating ground planes in the simulations.

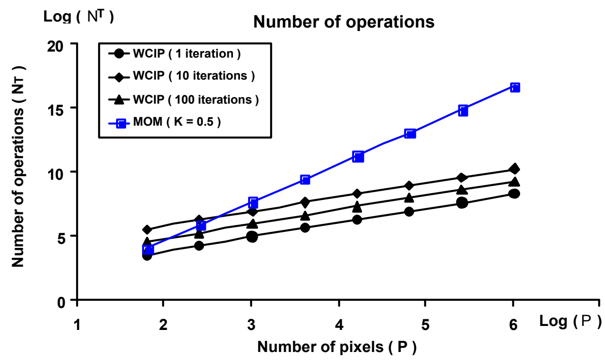

Fig. 7 Comparison of the number of operations between Moment method (K=0.5) and WCIP versus the number of iterations

V. Conclusion

WCIP which allows the description of complex and multi-layer design is seen properly conceived to apply to integrated circuit modeling without resorting to extensive computation times; it appears as an efficient alternative to the standard moment method in these 2.5D and 3D configurations. This method was applied to the analysis of the spiral inductors topologies including those requiring more than one metal level with patterned ground shield. The results were favorably compared to measurement and published results.

The WCIP method presented in this paper is expected to have wide applications in multi-layer IC's.

Acknowledgements

The authors would like to thank Philips-France in Caen for helpful discussions and supports and for providing measurements data.

References

[1] Joachim N.Burghartz, Keith A.Jenkins; "Multilevel-Spiral Inductors Using VLSI Interconnect Technology", *IEEE Electron Device Letters*, Vol. 17, No. 9, September 1996.

[2] M.Werthen, I.Wolff, Fellow, "Investigation of MMIC Inductor Coupling Effects", *IEEE MTT-S Intern. Symp. Digest.*, pp. 1793-1795., 1997.

[3] C.Patrick Yue, S.Simon Wong; "On-Chip Spiral Inductors with Patterned Ground Shields for Si-Based RF IC's", *IEEE Journal of Solid-State Circuit*, Vol. 33, No. 5, May 1998.

[4] Ali M. Niknejad, Robert G.Meyer, Fellow, "Analysis, Design and Optimization of Spiral Inductor and Transformers for Si RF IC's", *IEEE journal of solid-state circuit*, Vol. 33, No. 10, October 1998.

[5] Mina Danesh, john R. Long, R. A. Hadaway and D. L. Harame, "A Q-Factor Enhancement Technique For MMIC Inductor", *IEEE MTT-S Digest*, pp. 183-186, 1998.

[6] D.Bajon, H.Baudrand ; "Application of wave concept iterative procedure (WCIP) to planar circuits", *Microtec'2000*, Hannovre, pp. 864-868 , Septembre 2000.

[7] H.Baudrand "The Wave Concept in Electromagnetic Problems : Application in Integral Methods", *Asia Pacific Microwave Conference APMC'96*, New Dehli, 1996.